# Far-Infrared Spectra of $Al_2O_3$ Doped with Ti, V, and Cr*

R. R. JOYCE AND P. L. RICHARDS
*Inorganic Materials Research Division, Lawrence Radiation Laboratory, Department of Physics, University of California, Berkeley, California 94720*
(Received 12 November 1968)

The absorption spectrum of samples of $Al_2O_3$ doped with Ti, V, and Cr has been measured at 4.2°K over the frequency range 5–120 $cm^{-1}$ in applied magnetic fields up to 55 kOe. In $Al_2O_3$:Ti, absorption lines were observed at 37.8 and 107 $cm^{-1}$; these were due to transitions between the ground and first excited states of the $Ti^{3+}$ ion in a modified $Al_2O_3$ crystalline field. The Zeeman splitting of the observed lines yielded $g_{0\parallel}=1.11\pm0.03$, $g_{1\parallel}=2.00\pm0.06$, and $g_{0\perp}$, $g_{1\perp}<0.1$ for the ground and first excited states. Similar results were observed from the isoelectronic $V^{4+}$ ion in the $Al_2O_3$:V sample. Zero-field absorption lines were observed at 28.1 and 53 $cm^{-1}$, with $g$ values for the ground and first excited states of $g_{0\parallel}=g_{1\parallel}=1.43\pm0.04$ and $g_{0\perp}$, $g_{1\perp}<0.2$. The predicted energy levels of a single $d$ electron in the $Al_2O_3$ crystalline field modified by a dynamic Jahn-Teller effect are in satisfactory agreement with these data. An absorption line observed at 8.25 $cm^{-1}$ in $Al_2O_3$:V was attributed to the spin-orbit splitting of the lowest electronic state of the $V^{3+}$ ion. The Zeeman splitting of this line is in excellent agreement with the appropriate spin Hamiltonian with the parameters $g_{\parallel}=1.92\pm0.03$ and $g_{\perp}=1.74\pm0.02$. A 15-cm length of 1% $Al_2O_3$:Cr showed no absorption lines for any value of magnetic field, indicating that the transitions between the $Cr^{3+}$ ion-pair levels known to exist in this energy region are strongly forbidden. Samples of ruby reported to show far-infrared absorption lines were tested, and it was found that the splitting of the observed lines in a magnetic field was consistent with the assumption that they were due to $Ti^{3+}$ as an unintentional impurity.

## I. INTRODUCTION

In recent measurements of the far-infrared transmission of $Al_2O_3$ intentionally doped with Ti and V, Nelson *et al.*[1] and Wong *et al.*[2] observed absorption lines which they attributed to transitions between the electronic levels of $Ti^{3+}$ and $V^{4+}$ in the $Al_2O_3$ lattice. This assignment was reinforced by recent calculations made by Macfarlane *et al.*[3] of the expected energy levels of a single $d$ electron in the $Al_2O_3$ crystalline field modified by a dynamic Jahn-Teller effect. The lines attributed to $Ti^{3+}$ have a long history. Very similar lines were observed by Hadni[4] in a ruby sample with no suspected Ti impurity. The lines were then seen in Ti-doped $Al_2O_3$ by Perry *et al.*[5] More recently, Moser *et al.*[6] observed the same lines in samples of $Al_2O_3$ doped with Ti, Cr, and V. Since the line strengths did seem to correlate with analyses for Ti impurity, they were initially attributed to lattice vibrational modes. In order to resolve this discrepancy and to provide a critical test of the theory of single $d$ electrons in $Al_2O_3$, we have investigated the magnetic-field dependence of the far-infrared spectra of various samples of doped $Al_2O_3$. These included Ti-, V-, and Cr-doped material studied by Nelson[1] and by Wong[2] and Ti- and Cr-doped material used by Moser *et al.*[6] As will be discussed below, our results confirm the assignments to electronic transitions of $Ti^{3+}$ and $V^{4+}$ and are in reasonably good agreement with the theory.

We also investigated an absorption line near 8.25 $cm^{-1}$ in the sample of $Al_2O_3$:V which turned out to be due to a low-lying electronic level of the $(d)^2$ system of $V^{3+}$. Our magnetic-field results confirmed this assignment and could be fitted to the theoretical magnetic-field dependence obtained from a spin Hamiltonian.

## II. EXPERIMENTAL APPARATUS

The far-infrared data in this study were obtained using the techniques of Fourier-transform spectroscopy. In this method (which has been described fully elsewhere[7,8]), the spectrum is obtained by computing the Fourier transform of the interference pattern or interferogram measured using a two-beam interferometer. In practice, the interferogram is sampled at uniform intervals of $\Delta$, the path difference between the two beams, the Fourier integral is approximated by a sum, and the spectrum is computed on a high-speed digital computer. The resolution is limited only by the finite travel of the micrometer screw driving the moveable mirror; the our apparatus this is about 5 cm, corresponding to a maximum resolution of 0.10 $cm^{-1}$.

Figure 1 shows the far-infrared Michelson interferometer which we constructed for use in the frequency region 2–300 $cm^{-1}$. It is similar to the interferometer described by Richards,[8] except that the movable mirror is advanced by a stepping motor which is programmed to turn through a given angle of rotation each

* Work performed under the auspices of the U. S. Atomic Energy Commission.
[1] E. D. Nelson, J. Y. Wong, and A. L. Schawlow, Phys. Rev. **156**, 298 (1967).
[2] J. Y. Wong, M. J. Berggren, and A. L. Schawlow, J. Chem. Phys. **49**, 835 (1968).
[3] R. M. Macfarlane, J. Y. Wong, and M. D. Sturge, Phys. Rev. **166**, 250 (1968).
[4] A. Hadni, Phys. Rev. **136**, A758 (1964).
[5] C. H. Perry, R. Geick, and E. F. Young, Appl. Opt. **5**, 1171 (1966).
[6] J.-F. Moser, W. Zingg, H. Steffen, and F. K. Kneubühl, Phys. Letters **24A**, 411 (1967).
[7] J. Connes, Rev. Opt. **40**, 45 (1961); **40**, 116 (1961); **40**, 171 (1961); **40**, 231 (1961).
[8] P. L. Richards, in *Spectroscopic Techniques for Far Infra-Red, Submillimetre, and Millimetre Waves*, edited by D. H. Martin (North-Holland Publishing Co., Amsterdam, 1967), Chap. 2; J. Opt. Soc. Am. **54**, 1474 (1964).

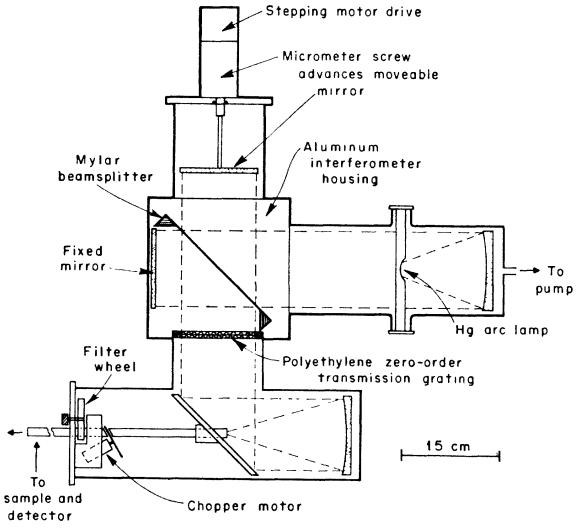


FIG. 1. Far-infrared Michelson interferometer used in the frequency range 2–300 $cm^{-1}$.

cycle. Three sets of filters can be used to remove unwanted radiation: Black polyethylene at the output of the interferometer removes visible and near-infrared light; polyethylene transmission gratings of the type described by Möller and McKnight[9] can be inserted as indicated in Fig. 1; a filter wheel of various Yoshinaga filters[10] is located at the output of the instrument. The output is chopped to permit lock-in detection and is conveyed to the sample through a 1.1-cm i.d. light pipe.

Figure 2 shows the cryostat, which contains the sample, superconducting magnet, and detector. The sample is mounted in a light pipe which can be removed from the cryostat, and samples can be changed without appreciable loss of He. The NbZr superconducting solenoid is capable of producing a field of 55 kOe. The chamber containing the In-doped Ge bolometer detector is separated from the sample cavity by a sapphire window and has its own liquid-He tank which can be pumped to provide the necessary low temperature for efficient bolometer operation. The signal from the bolometer is fed to a lock-in amplifier where it is converted to a dc voltage; the voltage is measured by a digital voltmeter and recorded on punched cards.

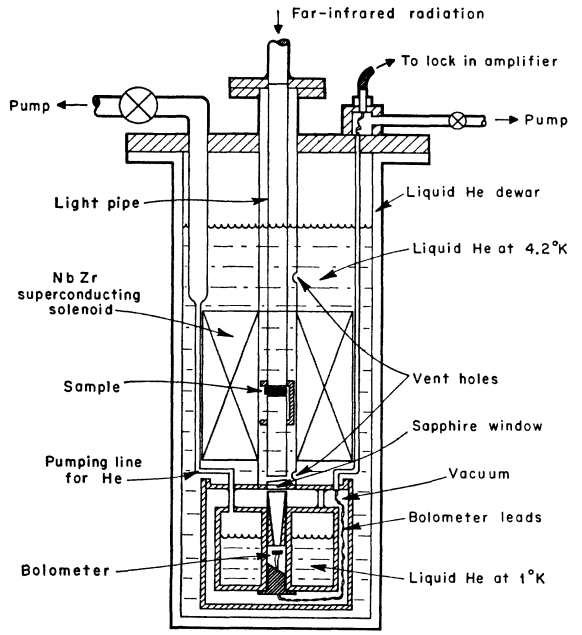


FIG. 2. Cryostat containing superconducting solenoid for transmission measurements in a magnetic field.

[9] K. D. Möller and R. V. McKnight, J. Opt. Soc. Am. **55**, 1075 (1965).

[10] Y. Yamada, A. Mitsuishi, and H. Yoshinaga, J. Opt. Soc. Am. **52**, 17 (1962).

## III. EXPERIMENTS WITH $Al_2O_3:Ti^{3+}$ AND $Al_2O_3:V^{4+}$

In the samples studied, the impurity ion is assumed to be substituted directly for an $Al^{3+}$ ion. The $Al^{3+}$ lattice symmetry is trigonal, but the six $O^{2-}$ ions adjacent to an Al site lie at the corners of a not too badly distorted octahedron; thus the crystalline field seen by an ion substituted for Al is largely cubic with a small trigonal distortion. For the case of the $d^1$ ions $Ti^{3+}$ and $V^{4+}$, this crystalline field splits the tenfold degenerate free-ion energy level of the $d$ electron into an upper level having $E_g$ symmetry and lower $A_{1g}$ and $E_g$ levels. In addition, the lower $E_g$ level is split by spin-orbit coupling and the upper $E_g$ level is split by the Jahn-Teller effect.[11] The resulting configuration is shown in Fig. 3. Only the three lowest levels, labeled $E_{3/2}$, $_1E_{1/2}$, and $_2E_{1/2}$ in order of increasing energy, are of interest in our experiment.

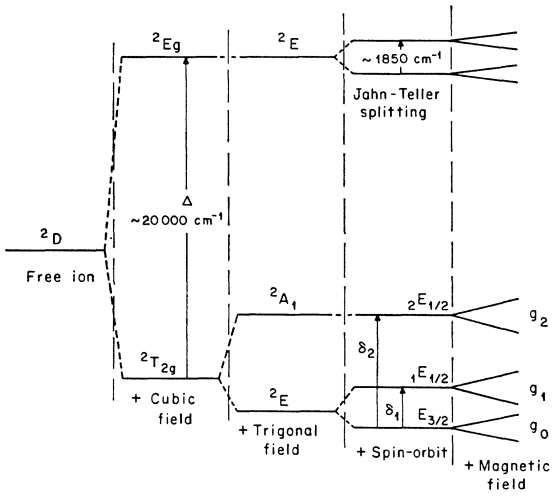


FIG. 3. Low-lying electronic energy levels of $Al_2O_3:d^1$.

[11] D. S. McClure, J. Chem. Phys. **36**, 2757 (1962).

The majority of our measurements were made on crystals of intentionally doped $Al_2O_3$:$Ti^{3+}$ and $Al_2O_3$:$V^{4+}$ which were immersed in liquid He to keep their temperature near 4.2°K. The Ti-doped samples were about 1 cm in diam and 1–5-mm thick. Some of them had the optic axis (referred to here as the $c$ axis) in the plane of the crystal (and thus perpendicular to the magnetic field), while others had the $c$ axis normal to the plane. By doing experiments on both types, we were able to orient our solenoidal magnetic field both parallel to and perpendicular to the $c$ axis. The concentration of Ti was 0.15% by weight of the oxide. It is not known how much of this was in the 3+ oxidation state. The $Al_2O_3$:$V^{4+}$ crystal was approximately a cube 1 cm on a side; experiments were done with the $c$ axis parallel to and perpendicular to the magnetic field. The concentration of V in the 3+ state in this sample was calculated by Slack[12] from optical absorption measurements to be about 0.06 wt%. Since the $V_2O_3$ structure (corresponding to $V^{3+}$) is the most stable state in the corundum lattice, the concentration of $V^{4+}$ was expected to be considerably smaller.

These samples were obtained from Wong and Schawlow and are similar to those used in their zero-field measurements.[1,2] Our zero-field measurements were consistent with their reported results. In the $Al_2O_3$:$Ti^{3+}$ sample, absorption lines were seen at 37.8 and 107 $cm^{-1}$. For the $Al_2O_3$:$V^{4+}$ sample, a similar pair of lines was observed at 28.1 and 53 $cm^{-1}$. For both samples the high-frequency line was sufficiently broader than the low-frequency line, so that observation of its Zeeman splitting would have been difficult in the available magnetic field. We therefore concentrated on the low-frequency lines at 37.8 $cm^{-1}$ in $Al_2O_3$:$Ti^{3+}$ and 28.1 $cm^{-1}$ in $Al_2O_3$:$V^{4+}$.

When a magnetic field was applied to the Ti-doped samples with $c\|H$, the 37.8 $cm^{-1}$ line split into four lines as indicated in Fig. 4. The effect of the thermal depopulation of the upper Zeeman level of the ground state at 4.2°K on the relative strengths of the Zeeman components was clearly seen. If we consider the ground ($E_{3/2}$) and first excited ($_1E_{1/2}$) states to have $g$ values of $g_0$ and $g_1$, respectively, then the transitions between them will have effective $g$ values of $g_a=\frac{1}{2}(g_0+g_1)$ and $g_b=\frac{1}{2}(g_0-g_1)$. We thus obtain parallel-field $g$ values of $g_{0\parallel}=1.11\pm0.03$ and $g_{1\parallel}=2.00\pm0.06$. For the samples with $c\perp H$, no broadening or splitting of the 37.8 $cm^{-1}$ line was observed, implying that the perpendicular-field $g$ values for both the ground and first excited states are less than 0.1.

The results for $Al_2O_3$:$V^{4+}$ were quite similar. The splitting of the 28.1-$cm^{-1}$ line in a field parallel to $c$ is shown in Fig. 5. The three-line pattern is a special case of the four-line pattern of Fig. 4 which occurs when the $g$ values of the two Zeeman split lines are the same. This interpretation is reinforced by the strength of the central line which was about twice that of the stronger of the two satellite lines. Our data indicate that $g_{0\parallel}=g_{1\parallel}=1.43\pm0.04$. With $c\perp H$, no splitting of the 28.1-$cm^{-1}$ line occurred, indicating $g_{0\perp}, g_{1\perp}<0.2$.

Our results for $g_0$ in both the Ti- and V-doped samples are in good agreement with previous results obtained

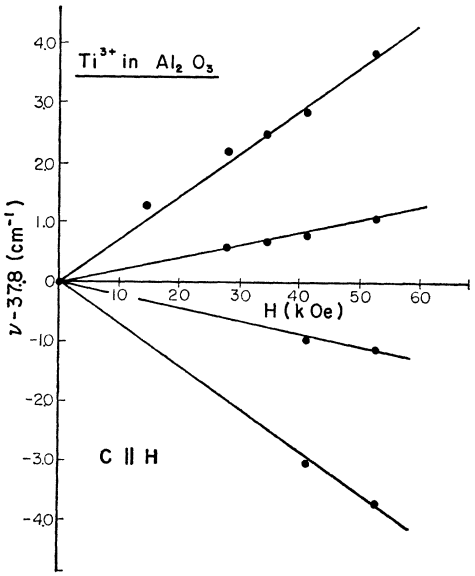


FIG. 4. Zeeman splitting of the 37.8-$cm^{-1}$ line in $Al_2O_3$:$Ti^{+}$ in a magnetic field oriented parallel to the optic axis. The points are averages of several measurements of the transmission minima.

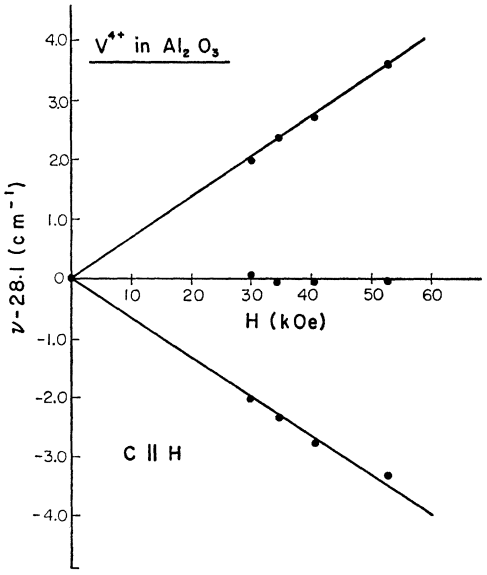


FIG. 5. Zeeman splitting of the 28.1-$cm^{-1}$ line in $Al_2O_3$:$V^{4+}$ in a magnetic field oriented parallel to the optic axis.

[12] G. A. Slack (private communication).

by electron paramagnetic resonance. Two groups[13,14] have measured values of $g_{0\parallel}=1.07$ and $g_{0\perp}<0.1$ for $Al_2O_3$:$Ti^{3+}$. Merritt[15] has recently measured a value of $g_{0\parallel}=1.39$ in $Al_2O_3$:$V^{4+}$.

## IV. THEORY OF $d^1$ ELECTRONIC STATES

Recently, Macfarlane *et al.*[3] considered the influence of a dynamic Jahn-Teller effect on the energy levels of a $d^1$ electronic system in the $Al_2O_3$ crystal symmetry. They found that the first-order effect uniformly reduced the matrix elements of the trigonal crystalline field and spin-orbit operators, whereas the inclusion of second-order effects introduced nonlinear corrections to the static crystalline-field results and allowed reasonable agreement with experimental data.

As shown in Fig. 3, the effect of the trigonal and spin-orbit operators on the $^2T_2$ octahedral level is a splitting of this sixfold degenerate level into three Kramers doublets $E_{3/2}$, $E_{1/2}$, and $_2E_{1/2}$. Using representative values for the trigonal and spin-orbit coupling parameters for $Al_2O_3$:$Ti^{3+}$, Macfarlane *et al.*, calculated the values $\delta_1=109$ cm$^{-1}$ and $\delta_2=771$ cm$^{-1}$, which are much larger than the experimental values of 37.8 and 107 cm$^{-1}$, respectively. Clearly, static crystal-field theory alone cannot account for the experimental observations.

The Jahn-Teller effect results from the coupling of an electronic system in a non-Kramers degenerate state to a nuclear displacement which lifts the degeneracy. The result is a displacement of the electronic system to a new position of minimum potential energy. The gain in the Jahn-Teller potential energy ($E_{JT}$) is balanced by the loss in elastic energy due to the displacement from the equilibrium position. For the octahedral $^2T_2$ level in $Al_2O_3$ there are three equivalent configurations to which the system can distort, and in the static Jahn-Teller effect the electronic system randomly occupies one of these three energy minima, provided $k_BT\ll E_{JT}$. When a perturbation to the octahedral field (such as a trigonal field or spin-orbit coupling) causes energy changes in the $^2T_2$ level which are comparable with $E_{JT}$, no such static distortion occurs, but the complex exhibits a coupled motion of the electrons and the lattice vibrational modes. This situation is referred to as the dynamic Jahn-Teller effect, and in the present case it causes a partial averaging of the trigonal and spin-orbit perturbations. To first order all matrix elements of these operators are reduced by a quenching factor $\gamma$ (Ham effect[16]). This first-order correction is insufficient to explain the experimental data, since the Ham effect would reduce the values of $\delta_1$ and $\delta_2$ by the same multiplicative factor, whereas the experimental values are, respectively, 0.35 and 0.14 of the estimated static crystalline-field values.

Macfarlane *et al.* then considered second-order perturbation effects within the manifold of basis states for the $^2T_2$ level and between the basis states for $^2T_2$ and those for $^2E$. They obtained analytical expressions for the energy splittings $\delta_1$ and $\delta_2$ as well as the $g$ values for the Zeeman splitting of the $E_{3/2}$, $E_{1/2}$, and $_2E_{1/2}$ levels. The independent variables involved are the trigonal and spin-orbit coupling parameters $v$ and $\zeta$, and the quenching factor $\gamma=\exp(-3E_{JT}/2\hbar\omega)$, where $\hbar\omega$ is the energy of the vibronic mode which is responsible for the Jahn-Teller effect.

The analytical expressions of Macfarlane *et al.* were fitted to our experimental data. Several results of the trial-and-error procedure used are tabulated in Table I, along with the data. The analytical expressions are quite complicated and are sufficiently sensitive to a small change in some of the variables to make the fit somewhat arbitrary. Two sets of theoretical parameters chosen primarily to fit the zero-field data for $\delta_1$ and $\delta_2$ are given in Table I to display this sensitivity.

## V. RUBY EXPERIMENTS

In 1964, Hadni observed absorption lines in ruby at 37 and 100 cm$^{-1}$, which he assigned to exchange coupling between pairs of $Cr^{3+}$ ions.[4] These pair lines have been observed optically, but the direct transition is between states of different spin and is forbidden. Nelson *et al.*[1] measured the far-infrared transmission of a sample of 1% $Cr_2O_3$ in $Al_2O_3$ which was 15 cm in length and observed no absorption lines. We repeated their experiment with the same sample and obtained similar negative results for all values of applied magnetic field. These results, as well as the similarity in frequency, width, and relative strength between the lines seen by Hadni and those subsequently found for $Ti^{3+}$ suggest strongly that he was seeing $Ti^{3+}$ as an unintentional impurity in his ruby.

Later, Moser *et al.*[6] reported lines at 37.75 and 108 cm$^{-1}$ in samples of $Al_2O_3$ doped with Ti, V, and Cr. These were attributed to lattice vibrational modes because the line strengths did not seem to correspond to those expected from analyses of the amount of Ti impurity present. However, the coincidence of their reported lines with the $Al_2O_3$:$Ti^{3+}$ spectrum and the lack of any lines in our sample of $Al_2O_3$:$Cr^{3+}$ raised doubts as to the correctness of this assignment. We performed transmission measurements on four of their samples (Nos. 4, 7, 13, and 14 listed in their Table I), all of which had Ti concentrations of less than 20 ppm by spectrographic analysis.[17] In agreement with their experiments, the 37.8-cm$^{-1}$ absorption was present in samples 7, 13,

[13] N. E. Kask, L. S. Kornienko, T. S. Mandel'shtam, and A. M. Prokhorov, Fiz. Tverd. Tela 5, 2306 (1963) [English transl.: Soviet Phys.—Solid State 5, 1677 (1964)].

[14] D. W. Feldman, D. C. Burnham, and J. G. Castle, Jr., Westinghouse Research Lab., Quarterly Scientific Report No. 4, 1964 (unpublished), under Contract No. AF 19(628)1640, AFCRL64-665.

[15] F. R. Merritt (private communication).

[16] F. S. Ham, Phys. Rev. 138, A1727 (1965).

[17] J. F. Moser, H. Steffen, and F. K. Kneubühl, Phys. Kondensierten Materie 7, 261 (1968).

TABLE I. Calculated and experimental values (in units of $cm^{-1}$) of the zero-field energy splittings $\delta_1$ and $\delta_2$ and the $g$ factors for the low-lying energy levels of the $d^1$ ions $Ti^{3+}$ and $V^{4+}$ in $Al_2O_3$. Comparison with experiment is made for several values of the crystalline-field parameters $v$ and $\zeta$ and the Jahn-Teller energy $E_{JT}$. Experimental results for the $d^2$ ion $V^{3+}$ are also listed.

| Sample | $v$ | $\zeta$ | $E_{JT}$ | $\delta_1$ | $\delta_2$ | $g_{0\parallel}$ | $g_{0\perp}$ | $g_{1\parallel}$ | $g_{1\perp}$ | $g_{2\parallel}$ |
|---|---|---|---|---|---|---|---|---|---|---|
| $Al_2O_3:Ti^{3+}$ | 700 | 120 | 200 | 44.98 | 104.21 | 1.16 | 0.0 | −2.22 | <0.2 | 1.88 |
| | 680 | 90 | 187 | 37.96 | 106.53 | 1.13 | 0.0 | −2.30 | <0.2 | 1.93 |
| | | Expt. | | 37.8 | 107 | 1.11 | <0.1 | −2.00 | <0.1 | |
| $Al_2O_3:V^{4+}$ | 970 | 195 | 320 | 27.93 | 53.15 | 1.59 | 0.0 | −2.00 | <0.5 | 1.86 |
| | 750 | 290 | 333 | 27.80 | 53.20 | 1.60 | 0.0 | −1.70 | <0.5 | 1.66 |
| $Al_2O_3:V^{3+}$ | | Expt. | | 28.1 | 53 | 1.43 | <0.2 | −1.43 | <0.2 | |
| | | Expt. | | $D=8.25\pm0.02$ $cm^{-1}$; $g_\parallel=1.92\pm0.03$; $g_\perp=1.74\pm0.02$ | | | | | | |

and 14, and the line strength measured did not correlate with the indicated concentration of Cr, Ti, or V. In the cases where the 37.8-$cm^{-1}$ line was observed, it exhibited a Zeeman splitting consistent with the assumption that it was due to $Ti^{3+}$.

In addition, a 1-cm-thick 1.2% ruby of Swiss origin was found to have strong absorptions at 37.8 $cm^{-1}$ (with a peak absorption coefficient $\alpha\sim2.4$ $cm^{-1}$) and 107 $cm^{-1}$ ($\alpha\sim0.8$ $cm^{-1}$) which split in a manner indicating $Ti^{3+}$. Spectrographic analysis indicated a Ti concentration $\sim100$ ppm, and the line strength was at least ten times the minimum observable value.

The lack of good correlation between the 37.8-$cm^{-1}$ line strength and the Ti concentration given by spectrographic analysis is probably the result of a variation from sample to sample of the fraction of Ti in the 3+ oxidation state. The use of spectrographic analysis as an indicator of $Ti^{3+}$ concentration is therefore of questionable value, because it can provide no more than an upper limit. The proportion of Ti in the 3+ state will depend upon the conditions under which the crystal was grown and aspects of its past history, such as exposure to radiation which can oxidize some $Ti^{3+}$ into $Ti^{4+}$. The possibility also exists that the transition probability for a given ion may depend on the presence of defects or other ions (such as Cr) in close proximity.

## VI. $Al_2O_3:V^{3+}$ EXPERIMENTS

The $V^{3+}$ ion has two $d$ electrons, and the effect of the $Al_2O_3$ crystalline field on the free-ion $^3F$ state, shown in Fig. 6, is more complicated than for $V^{4+}$. Only the lowest level ($^3A_2$) is of interest here, since the trigonal splitting is believed[18] to be $\sim1200$ $cm^{-1}$, so that the mixing between the $^3A_2$ and $^3E$ states is small.

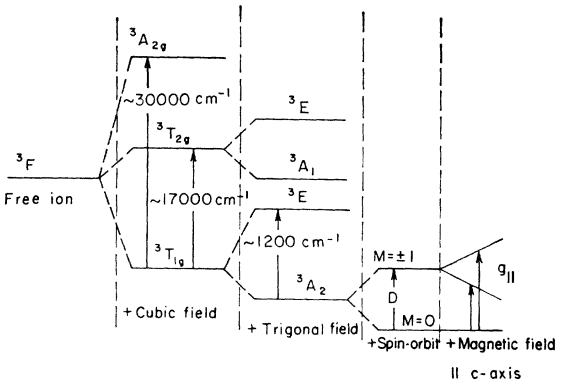


FIG. 6. Low-lying electronic energy levels of $Al_2O_3:d^2$.

The sample was the same one used for the $Al_2O_3:V^{4+}$ experiments, and all measurements were done with the sample at 4.2°K. For no applied field, a strong line with a peak absorption coefficient $\alpha\sim1.5$ $cm^{-1}$ was observed at 8.25 $cm^{-1}$. In a field parallel to the $c$ axis, this line split linearly with field. When the field was applied perpendicular to the $c$ axis, a quadratic Zeeman effect was observed. Figure 7 shows the behavior of the 8.25-$cm^{-1}$ line in both field orientations.

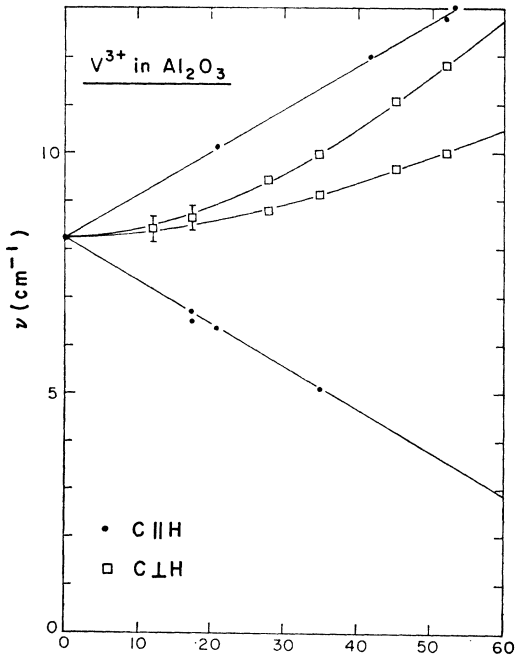


FIG. 7. Zeeman splitting of the 8.25-$cm^{-1}$ line in $Al_2O_3:V^{3+}$. The circles and squares indicate experimental values for the magnetic field oriented, respectively, parallel to and perpendicular to the optic axis. Except where incicated by flags, the linewidth at one-half the peak absorption coefficient is $\sim0.3$ $cm^{-1}$.

[18] A. Abragam and M. H. L. Pryce, Proc. Roy. Soc. (London) **A205**, 135 (1951).

If we consider the ground ($^3A_2$) state only the magnetic properties can be described by means of the spin-Hamiltonian

$$\mathcal{H}=DS_z'^2+g_{\parallel}\beta S_z'H_z+g_{\perp}\beta(S_x'H_x+S_y'H_y),$$

where $S'$ is the effective spin of the ground state ($|S'|=1$). Because of the large trigonal splitting and the small spin-orbit splitting very little mixing between the spin states of $^3A_2$ and those of higher levels is expected, so the spin states $|+\rangle$, $|0\rangle$, and $|-\rangle$ are reasonably good basis states for $^3A_2$. Any mixing will tend to quench the Zeeman splitting of the $^3A_2$ level, however, giving values of $g_{\parallel}$ and $g_{\perp}$ smaller than 2.0 by an amount which depends on the ratio of the spin-orbit coupling to the trigonal splitting.[18]

The first term in $\mathcal{H}$ splits the $^3A_2$ level into two levels separated by $D$, the doubly degenerate $M=\pm1$ level lying higher. The effect of a magnetic field parallel to $c$ is represented by the second term; this perturbation does not mix states of different $M$ and the $M=\pm1$ level is split by $2g_{\parallel}\beta H$, as shown in Fig. 6. The third term in $\mathcal{H}$ represents a magnetic field perpendicular to $c$, which mixes the three spin states. The resulting transitions start out at $D$ and both curve upward as the field increases. Figure 7 shows the experimental data (points) and the theoretical results (lines) obtained by adjusting $g_{\parallel}$ and $g_{\perp}$ for the best fit. An excellent fit is obtained for both field orientations which yields the results $g_{\parallel}=1.92\pm0.03$ and $g_{\perp}=1.74\pm0.02$.

Our direct measurement of the transitions determines all three parameters in the spin Hamiltonian to a high degree of precision. A recent microwave-absorption experiment[19] yielded the results $D=8.26\pm0.01$ cm$^{-1}$ and $D=8.27\pm0.01$ cm$^{-1}$ by two different techniques. Within the limits of our experiment, we find $D=8.25\pm0.02$ cm$^{-1}$. Electron paramagnetic resonance experiments[20,21] have obtained the respective results $g_{\parallel}=1.915$ and $g_{\parallel}=1.910$, in excellent agreement with our values. Smith and Mires[22] have recently measured $g_{\perp}=1.74\pm0.01$ by a torque method.

## VII. CONCLUSIONS

From our experiments on $Al_2O_3$:$Ti^{3+}$ and $Al_2O_3$:$V^{4+}$ we conclude that the observed absorption lines are due to low-lying electronic states of the nominal impurity ion in the effective crystalline field of the host lattice. The Zeeman splitting of the low-frequency absorption line in each case shows that they cannot be due to lattice vibrational modes. The general agreement of our results with the theory of Macfarlane *et al.*, leads to the conclusion that the vibronic interaction correction to the static crystalline field can largely explain the electronic levels of a $d^1$ impurity ion in $Al_2O_3$. As shown in Table I, the agreement between theory and experiment is not perfect. Since our fit was made by adjustment of the parameters to fit only two of the five variables ($\delta_1$ and $\delta_2$), there is considerable freedom of choice for the values of several parameters. We found that the value of $g_{0\parallel}$ was rather insensitive to changes in the trigonal and spin-orbit parameters, and the 10% disagreement between experimental and theoretical values of $g_{0\parallel}$ for $Al_2O_3$:$V^{3+}$ indicates that improvement of the theory is desirable. It seems likely that further improvement can be expected if the interaction with the lattice is included a more complete way. This would seem especially necessary to understand the large transition probability for the 37.8-cm$^{-1}$ transition of $Ti^{3+}$.

Our experiments on $Al_2O_3$:$V^{3+}$ are in agreement with previous work and yield precise values of all three spin-Hamiltonian parameters.

## ACKNOWLEDGMENTS

We are grateful to Professor A. L. Schawlow and Dr. J. Y. Wong for providing the samples of $Al_2O_3$:Ti, $Al_2O_3$:V, and $Al_2O_3$:Cr used in our experiments, and to Dr. R. M. Macfarlane and Dr. J. Y. Wong for helpful discussions and for making their calculations available to us prior to publication. Thanks are also due Dr. J. F. Moser and Dr. F. K. Kneubühl for allowing us to measure their samples and Dr. G. A. Slack for suggesting the investigation of the $V^{3+}$ line.

[19] E. A. Vinogradov, N. A. Irisova, T. S. Mandel'shtam, A. M. Prokhorov, and T. A. Shmaonov, Pis'ma v Redaktsiyu **4**, 373 (1966) [English transl.: Soviet Phys.—JETP Letters **4**, 252 (1966)].

[20] G. M. Zverev and A. M. Prokhorov, Zh. Eksperim. i Teor. Fiz. **40**, 1016 (1961) [English transl.: Soviet Phys.—JETP **13**, 714 (1961)].

[21] M. Sauzade, J. Pontnau, P. Lesas, and D. Silhouette, Phys. Letters **19**, 617 (1966).

[22] A. R. Smith and R. W. Mires, Phys. Rev. **172**, 265 (1968).